Optical and Quantum Electronics **23** *(1991) 639–647*

Induced steepening of femtosecond pulses

S. G. DINEV, A. A. DREISCHUH
Department of Physics, Sofia University, BG-1126, Sofia, Bulgaria

Received 30 July; accepted 17 December 1990

The femtosecond pulse conversion to the XUV has been studied theoretically for the first time in a gas-filled waveguide, including the influence of the pump-induced phase modulation on the phase matching conditions, waveguide propagation and signal pulse shape. The conversion of femtosecond pulses from excimer amplifiers to the range of 83 nm to 88 nm is discussed

1. Introduction

A subpicosecond pulse generation is required for the study of phenomena with high temporal resolution. Ultrashort pulses in the XUV and X-ray range would allow such measurements in solid state- and plasma physics [1, 2]. The self-phase modulation (SPM) and compression [3, 4] is widely used in the visible range, however due to the relatively small peak intensity in the XUV and the soft X-ray region [5, 6] the method seems to be unapplicable.

In the last few years has been considerable progress in the study of induced-phase modulation (IPM) as an alternative of SPM [7–10]. Another method for short pulse generation in the XUV is the nonlinear conversion from the UV. Some of the shortest UV pulses reported in the literature are 43 fs at $\lambda = 310$ nm [11], 170 fs at $\lambda = 308$ nm [12] and 60 fs at $\lambda = 248$ nm [13].

The aim of the present work is to study the four-wave mixing of femtosecond and picosecond pulses, both in the UV range. Noncolinear phase matching in a gas-filled waveguide is used and the influence of IPM on different aspects of the up-conversion process are discussed.

2. Theoretical description

2.1. Four-wave mixing

Assuming Gaussian input pulses

$$I_{1,2} = I_{1,2_0} \exp(-t^2/\tau_{1,2}^2) \tag{1}$$

the signal-wave intensity in the phase matched process $\omega_s = 2\omega_1 + \omega_2$ according to the plane-wave approximation is given by [14]

$$\begin{aligned} I_s(\eta, z) = {} & \pi(32\pi^3 10^7 I_{1_0} N \chi_T^{(3)})^2 I_{2_0}/[4a(c\lambda_s n_1)^2 n_2 n_s] \\ & \times \exp\{-\eta^2\{[(2/\tau_1^2) + (1/\tau_2^2)] - (1/a)[(2v_{13}/\tau_1^2) + (v_{23}/\tau_2^2)]^2\}\} \\ & \times [\Phi(a^{1/2}z - b/a^{1/2}) + \Phi(b/a^{1/2})]^2 \end{aligned} \tag{2}$$

0306–8919/91 $03.00 + .12

where z is the longitudinal distance, N is the particle density and c is the velocity of light, $\Phi(x) = (2/\pi^{1/2}) \int_0^x \exp(-y^2)\,dy$ is the probability integral

$$b = \eta[(2v_{1s}/\tau_1^2) + (v_{2s}/\tau_2^2)] \qquad a = 2[(2v_{1s}^2/\tau_1^2) + (v_{2s}^2/\tau_2^2)]$$

$$\eta = t - (z/u_s) \qquad v_{I,J} = (1/u_I) - (1/u_J)$$

I_1, I_2, I_s and n_1, n_2, n_s are the intensity and the refractive indices at the frequencies ω_1, ω_2, ω_s, respectively, and u_1, u_2, u_s are the respective group velocities.

Under two-photon resonant conditions the nonlinear susceptibility $\chi_T^{(3)}$ can be presented in the form [15]

$$\chi_T^{(3)}(\omega_s;\, \omega_1,\, \omega_1,\, \omega_2) \approx (\omega_R - 2\omega_1)^{-1} \chi_F^{(3)}(\omega_s) \tag{3}$$

where $\chi_F^{(3)}(\omega_s)$ is real and includes the nonresonant contribution to the $\chi_T^{(3)}(\omega_s)$, whereas the resonant denominator has a real and imaginary part. For Maxwellian velocity distribution of the particles and Gaussian pump intensity distribution in the frequency scale, when

$$\gamma \gg \gamma_D \tag{4}$$

$$\gamma^2/4 + \Delta\omega^2 \gg \gamma_D^2/2 + \delta^2/8$$

(γ, γ_D are the resonant and Doppler linewidths, respectively, $\Delta\omega$ is the pump laser detuning from resonance and δ is the laser linewidth), Equation 2 can be rewritten in the form [15]

$$I_s(z, \eta) = [4C/(\Delta\omega^2 + \gamma^2/4)^2] \times \{1 - [\gamma_D^2/(\Delta\omega^2 + \gamma^2/4)] + [(3\Delta\omega^2 - \gamma^2/4)(\gamma_D^2 + \delta^2/4)/(\Delta\omega^2 + \gamma^2/4)^2]\} \tag{5}$$

where

$$C = \pi(32\pi^3 10^7 I_{1_0} N \chi_F^{(3)})^2 I_{2_0}/[4a(c\lambda_s n_1)^2 n_2 n_s] \times \exp\{-\eta^2\{[(2/\tau_1^2) + (1/\tau_2^2)] - (1/a)[(2v_{13}/\tau_1^2) + (v_{23}/\tau_2^2)]^2\}\} \times [\Phi(a^{1/2}z - b/a^{1/2}) + \Phi(b/a^{1/2})]^2 \tag{6}$$

Generally speaking, τ_1, τ_2 and δ are not constants and depend on the longitudinal coordinate z.

Assuming that self-phase modulation of the pump is the only nonlinear effect at frequencies ω_1 and ω_2, the change in the τ_1, τ_2 and δ with the length can be evaluated using the results of the variational approach [16]

$$\frac{d^2\tau_{1,2}}{dz^2} = 4\alpha^2(\omega_{1,2})\tau_{1,2}^{-2} - 2^{1/2}\alpha(\omega_{1,2})k_{\omega_{1,2}}^{SPM}(z)\,|A_{1,2}|^2\tau_{1,2}^{-2} \tag{7a}$$

$$b_{\omega_1}(z) = -[4\alpha(\omega_1)\tau_1(z)]^{-1}\frac{d\tau_1}{dz} \tag{7b}$$

$$\delta(z) = \max\begin{cases}\delta(z=0) \\ 2^{1/2}\ln(2) b_{\omega_1}(z)\tau_1(z)\end{cases} \tag{7c}$$

where α and k^{SPM} are coefficients, determined from the dispersion and self-phase modulation and $b(z)$ is the frequency-chirp parameter.

In our view, this is a more precise description of the four-wave mixing process, taking into account better the parameters of the media and the pump. Particularly involved are the pulse walk-off, the symmetrical temporal broadening and the self-phase modulation of the pump.

2.2. Pump-induced steepening of the signal

It has already been shown, that the presence of a strong primary signal can induce deformation of the pulse shape of a weak second harmonic signal in a medium with cubic nonlinearity [17]. The signal generation and pump-induced steepening we treat as separate steps, although in general, they occur simultaneously. This is a good approximation as long as the change of the pulse is small.

Let us start from the equation, describing the IPM on a weak signal from an intense pulse, propagating simultaneously with the first one [10]

$$i\frac{\partial A_s}{\partial z} + \alpha_s \frac{\partial^2 A_s}{\partial \eta^2} + k^{IPM}(\omega_s)|A_p|^2 A_s + i\beta \frac{\partial}{\partial \eta}(|A_p|^2 A_s) = 0 \tag{8}$$

where α_s and $k^{IPM}(\omega_s)$ are coefficients, determined from the dispersion and the induced phase modulation and the term comprising β reflects the shock-wave of the envelope [18]. Let the field amplitudes be described by expressions of the type

$$A_s = A_{s0}(z)\exp[-(\eta - \xi)^2/2\tau_s^2(z)]\exp(i\Phi_s) \tag{9a}$$

$$A_P = A_{P0}(z)\exp[-\eta^2/2\tau_P^2(z)]\exp(i\Phi_P) \tag{9b}$$

where $\Phi_s(z, \eta)$ and $\Phi_P(z, \eta)$ are phase terms and ξ is the shift of the signal pulse peak. Following the approach applied by the SPM [18], substituting Equation 9 into Equation 8 and separating the real and imaginary parts, for the case of zero group velocity dispersion at the signal frequency we get

$$\xi = \beta A_P^2 z, \tag{10a}$$

i.e.

$$I_s = I_s(z, \eta = 0)\exp[-(\eta - \beta A_P^2 z)^2/\tau_s^2(z)] \tag{10b}$$

As seen from Equation 10b, inducing shock waves on the signal, its peak has a velocity, different from the group velocity

$$u_{s_{PEAK}} = u_s/(1 + u_s\beta|A_p|^2) \tag{10c}$$

where

$$\beta = 6\pi N\chi^{(3)}_{IPM}(\omega_s; \omega_s, \omega_P, -\omega_P)/(cn_s) \tag{10d}$$

In our case

$$\xi = 6\pi Nz[\chi^{(3)}_{IPM}(\omega_s; \omega_s, \omega_1, -\omega_1)A_1^2(\eta - zv_{1s}, z) + \chi^{(3)}_{IPM}(\omega_s; \omega_s, \omega_2, -\omega_2)A_2^2(\eta - zv_{2s}, z)]/(cn_s) \tag{11}$$

3. Numerical results and discussion

The medium under consideration is a hollow Al waveguide with internal diameter 10 μm, filled with XeI as a nonlinear medium. The wavelength $\lambda_1 = 249.6$ nm (second harmonic of a dye laser) is chosen to be near a two-photon resonance with the $5p^6$–$6p[1/2]_0$ transition

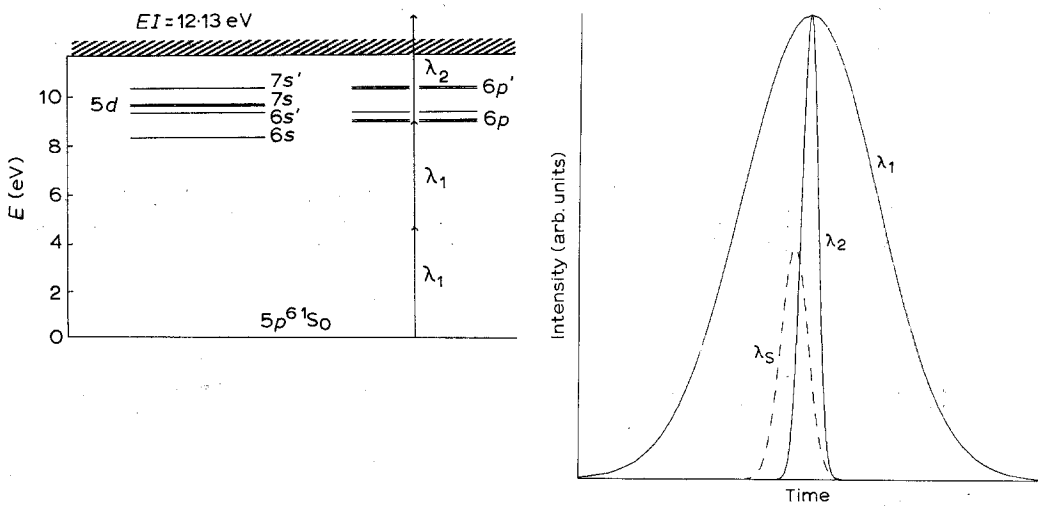

Figure 1 (a) Simplified energy-level diagram of Xe and (b) distribution of the pulses in the medium.

in XeI (Fig. 1a). The disposition of the pulses in the medium is shown in Fig. 1b. For the pressures considered 1 and 5 atmospheres Equation 4 is fulfilled. We consider femtosecond pulses from excimer amplifiers as a last stage at $\lambda_2 = 248\,\text{nm}$ ($\tau_2(z = 0) = 60\,\text{fs}$ [13]) and $\lambda_2 = 308\,\text{nm}$ ($\tau_2(z = 0) = 170\,\text{fs}$ [12]). Some important parameters, included in the model, are presented in Table I and Table II. The maximum pump powers are limited by

TABLE I Model parameters for conversion of femtosecond pulses in the XUV ($\lambda_s = 83.02\,\text{nm}$) and the induced shock wave.

Parameter	Unit	Value	
		$\lambda_1 = 249.6\,\text{nm}$	$\lambda_2 = 248\,\text{nm}$
τ (FWHM)	s	2×10^{-11}	6×10^{-14}
n	–	0.997793	0.997831
u	cm s^{-1}	2.989211×10^{10}	2.989331×10^{10}
$\sigma^{(1)}$	cm^2	7.47×10^{-22}	7.37×10^{-22}
$\sigma^{(2)}$	$\text{cm}^4\,\text{W}^{-1}$	3.8×10^{-31}	1.8×10^{-34}
I_{MAX}	W cm^{-2}	4.7×10^{7}	1.9×10^{11}
I	W cm^{-2}	4.7×10^{6}	10^{8}
$\chi^{(3)}_{SPM}$	esu	8.5×10^{-34}	-6.6×10^{-35}
$\chi^{(3)}_{IPM}(\omega_s, \omega_P)$	esu	-1.5×10^{-30}	-9×10^{-29}
$\chi^{(3)}_T$	esu	5.4×10^{-33}	
λ_s	nm	83.02	
u_s	cm s^{-1}	2.996949×10^{10}	
n_s	–	0.999501	
n_s^{L+NL}	–	0.99717	
z	cm	3	
N	cm^{-3}	2.5×10^{19}	
I_s	W cm^{-2}	1.91×10^{5}	
τ_s (FWHM)	s	2×10^{-13}	
θ_1	deg	4.3	
θ_2	deg	1.5	

TABLE II Model parameters for conversion of femtosecond pulses in the XUV (λ_s = 88.81 nm) and the induced shock wave.

Parameter	Unit	Value
		λ_2 = 308 nm
τ (FWHM)	s	1.7×10^{-13}
n	–	0.996227
u	cm s^{-1}	2.982948×10^{10}
$\sigma^{(1)}$	cm^2	1.24×10^{-21}
$\sigma^{(2)}$	cm^4 W^{-1}	2.9×10^{-36}
I_{MAX}	W cm^{-2}	1.9×10^{11}
I	W cm^{-2}	10^8
$\chi^{(3)}_{SPM}$	esu	7.6×10^{-36}
$\chi^{(3)}_{IPM}(\omega_s, \omega_1)$	esu	-2×10^{-31}
$\chi^{(3)}_{IPM}(\omega_s, \omega_2)$	esu	-4.6×10^{-29}
$\chi^{(3)}_I$	esu	5.3×10^{-33}
λ_s	nm	88.81
u_s	cm s^{-1}	2.995109×10^{10}
n_s	–	0.999377
n_s^{L+NL}	–	0.981202
z	cm	3
N	cm^{-3}	2.5×10^{19}
I_s	W cm^{-2}	2.23×10^5
τ_s (FWHM)	s	4×10^{-13}
θ_1	deg	22.6
θ_2	deg	6.7

self-focusing and/or breakdown in the gas. The matrix elements for the bound–bound transitions are from Radzig and Smirnov [19] and for bound-free transitions, from Peach [20]. The nonlinear susceptibilities are calculated according to the single-sided Fineman diagrams [21]. The accuracy of calculation, according to the accuracy of the matrix elements used, is $\approx 50\%$. It can be shown, that the calculated $\chi^{(3)}_{SPM}$ values are low enough and the SPM and self-steepening of the pump pulses are negligible for the pump intensities considered.

In a previous paper we have studied the influence of the cross-phase modulation effects on the phase-matching condition [22]. In principle, the high negative values of $\chi^{(3)}_{IPM}(\omega_s; \omega_s, \omega_P, -\omega_P)$, determined by the small detuning of $2\omega_1$ from the two-photon resonance, permits us to compensate the positive wave-vector mismatch, however it strongly limits the pump intensities. In our model we use a noncolinear phase matching [23] at higher pump intensities. The phase matching angles θ_1 (between the wave-vectors k_1 and k_2) and θ_2 (between k_1 and k_s) (see Table I, Table II) satisfy the conditions for waveguide propagation in the aluminium capillary (n_{Al} ($\lambda \approx 88$ nm) ≈ 0.67 [24]). It should be noted that this is a nonconventional use of the vector phase matching, applied to FWFM with sum-frequency generation in a medium with a positive dispersion. The high value of $\chi^{(3)}_{IPM}(\omega_s)$ indicates a pump-induced defocusing of the signal, however the angle of defocusing is considerably smaller, compared to the critical angle for waveguide distribution in our case. Tables I and II give the calculated single- and two-photon absorption cross-sections $\sigma^{(1)}$ and $\sigma^{(2)}$, respectively.

Let us consider the case λ_2 = 248 nm and λ_s = 83.02 nm (Table I). Plotted in Fig. 2 is the signal intensity as a function of time for a capillary length 1 cm, 2 cm and 3 cm

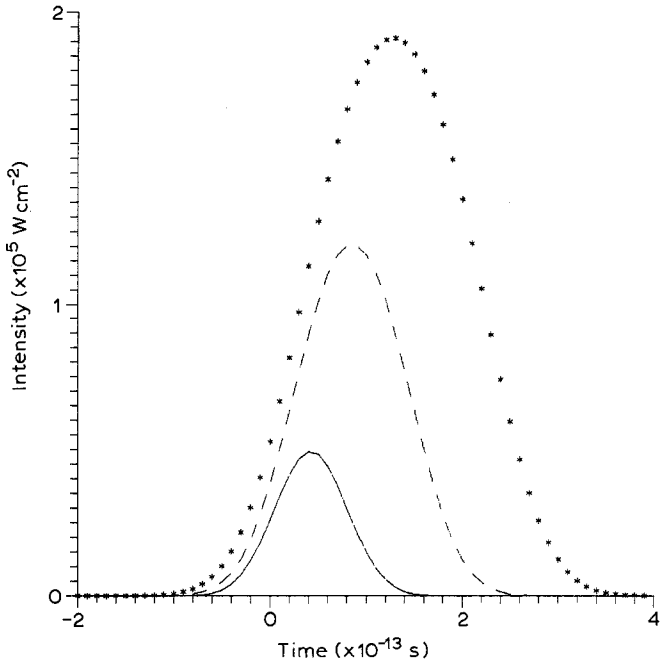

Figure 2 Signal intensity versus time for capillary length z = 1 cm (——), 2 cm (– – –) and 3 cm (∗∗∗). (λ_s = 83.02 nm; N_{Xel} = 2.5 × 10^{19} cm^{-3}.

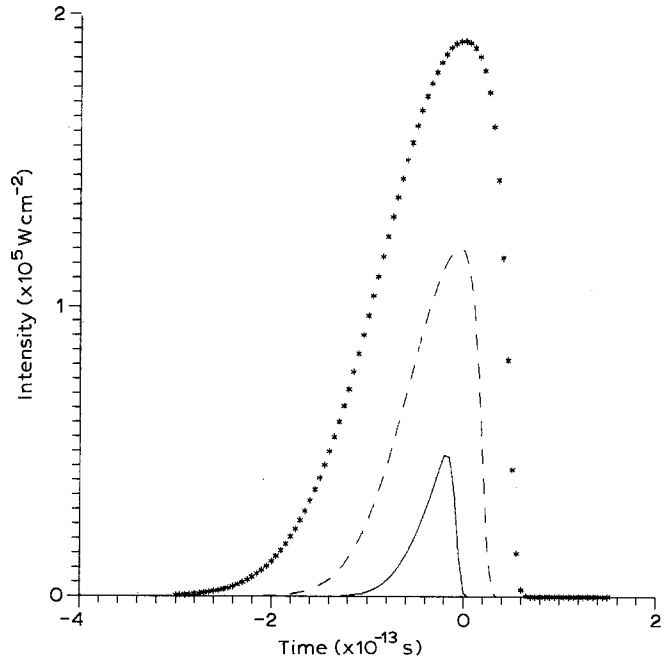

Figure 3 Signal intensity versus time including pump-induced steepening (λ_s = 83.02 nm, N_{Xel} = 2.5 × 10^{19} cm^{-3}, z = 1 cm (——), 2 cm (– – –) and 3 cm (∗∗∗).

($N = 2.5 \times 10^{19}\,\mathrm{cm}^{-3}$; $\tau_s = 200\,\mathrm{fs}$ FWHM), calculated according to Equations 5–7. The pulses have a Gaussian form. The leading front of the signal pulse, due to group velocity mismatch, moves ahead of the femtosecond pump pulse and is amplified less than the trailing edge. Due to the proximity of λ_1 and λ_2, $v_{12} \approx 0$ and the Gaussian form is described by the terms in Equation 6, containing the probability integral. The induced shock wave on the signal, involving Equations 10 and 11, is shown in Fig. 3. The pumping picosecond pulse causes a nearly constant change in the velocity of all parts of the signal pulse while the femtosecond pump pulse accelerates the trailing edge. Under their combined action the leading front remains Gaussian, while the trailing edge is steepened.

To investigate the influence of the particle density we have modelled the same case for $N = 1.2 \times 10^{20}\,\mathrm{cm}^{-3}$ and waveguide length 1 cm (Fig. 4). Under the joint action of the dispersion and two-photon absorption at λ_1 the signal at the waveguide output is deformed in super-Gaussian form

$$I_s = I_{s_0} \exp[-(\eta/\tau_s)^{2m}],$$

where $m = 2$ and the pulse duration is $\tau_s \approx 290\,\mathrm{fs}$. Qualitatively, the change in the signal pulse form taking into account the induced shock wave is similar (Fig. 5). The small peak, lagging behind the trailing edge of the signal, is a part of it, hitting the trailing edge of the femtosecond pump pulse.

Shown in Table II are the parameters of the model for conversion of a 170 fs pulse at $\lambda_2 = 308\,\mathrm{nm}$ to the XUV $\lambda_s = 88.81\,\mathrm{nm}$ ($N = 2.5 \times 10^{19}\,\mathrm{cm}^{-3}$). For comparison, we plot in Fig. 6 the signal pulse form at the capillary output ($L = 3\,\mathrm{cm}$), with (solid line) and without (dotted line) the shock wave. The changes in the pulse form discussed above are clearly seen.

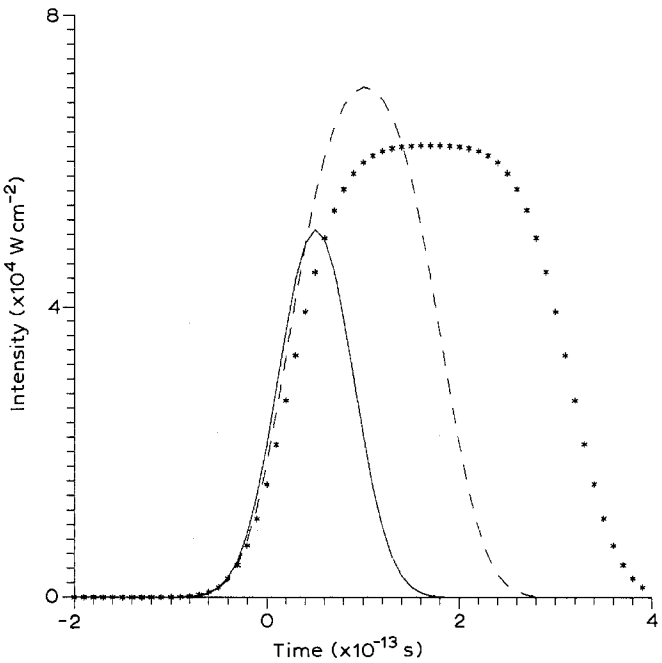

Figure 4 Signal intensity ($\lambda_s = 83.02\,\mathrm{nm}$) against time for $N_{Xe} = 10^{20}\,\mathrm{cm}^{-3}$ at $z = 0.3\,\mathrm{cm}$ (——), 0.6 cm (– – –) and 1 cm (* * *).

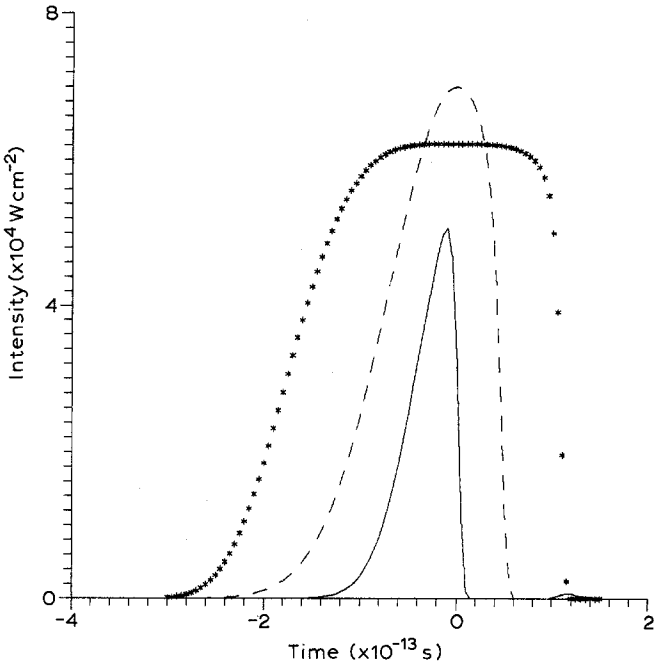

Figure 5 Pump-induced steepening of the signal (λ_s = 83.02 nm) for N_{Xe} = 10^{20} cm^{-3} at z = 0.3 cm (——), 0.6 cm (– – –) and 1 cm (* * *).

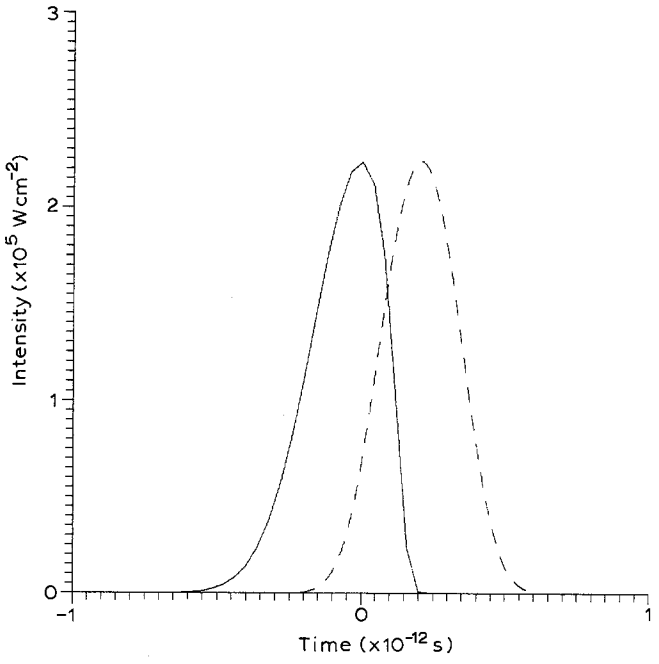

Figure 6 Signal shape (λ_s = 88.81 nm) at the output of the capillary (z = 3 cm) with (——) and without pump-induced steepening (– – –).

As far as the experimental verification is concerned, we are not aware of a medium to measure the third-order correlation function and thus, the asymmetry of the signal pulse. It could be performed in our view, with an X-ray streak camera or using a signal generated in a longer waveguide ($\approx 10\,\text{cm}$), respectively more dense medium to get $\tau_s \geqslant 1\,\text{ps}$. The use of waveguides with the lowest possible internal diameter is desirable, because the multimodal temporal dispersion can change the shape of the XUV-pulses significantly and wash-out the induced-steepening effect described.

The high values of $\chi^{(3)}_{\text{IPM}}$ also indicate a chirp induced on the signal. However, we would not comment now on the possibility for pulse compression. A detailed study is needed to find the dependence of pulse shape on the linear and nonlinear chirp, as well as knowledge of the characteristic response-time for IPM through the continuum. Theoretical considerations on this problem for the SPM- and IPM-processes are already published [25, 26].

4. Conclusions

In this paper we have studied, for the first time to our knowledge, the generation of femtosecond pulses in the XUV range using noncolinear phase matching in the FWSM in a medium with positive dispersion. The analyses show that the IPM influences the phase-matching conditions and the waveguide propagation, and deforms the signal pulse shape. In model calculations we have studied the generation of pulses at $\lambda_s = 83.02\,\text{nm}$ with a duration of $\tau_s = 200\,\text{fs}$ and intensity $I_s = 1.9 \times 10^5\,\text{W cm}^{-2}$, and also $\lambda_s = 88.81\,\text{nm}$ with a duration of $\tau_s = 400\,\text{fs}$ and intensity $I_s = 2.2 \times 10^5\,\text{W cm}^{-2}$.

References

1. D. G. STEARNS, O. L. LANDEN, E. M. CAMPBELL and J. H. SCOFIELD, *Phys. Rev.* **A37** (1988) 1684.
2. W. K. POPOV, *Sov. Phys. Usp.* **147** (1985) 587.
3. C. V. SHANK, R. L. FORK, R. YEN, R. H. STOLEN and W. J. TOMLINSON, *Appl. Phys. Lett.* **40** (1982) 761.
4. D. GRISCHKOWSKY and A. C. BALANT, *ibid.* **41** (1982) 1.
5. J. REINTJES, *Appl. Opt.* **19** (1980) 3889.
6. V. O. PAPANYAN and M. BERTOLOTTI, *IEEE J. Quantum Electron.* **QE-23** (1987) 551.
7. P. L. BALDECK, R. R. ALFANO and G. P. AGRAWAL, *Appl. Phys. Lett.* **52** (1988) 1939.
8. J. T. MANASSAH, *Opt. Lett.* **13** (1988) 755.
9. G. P. AGRAWAL, P. L. BALDECK and R. R. ALFANO, *ibid* **14** (1989) 137.
10. R. R. ALFANO, P. L. BALDECK, P. P. HO and G. P. AGRAWAL, *J. Opt. Soc. Amer.* **B6** (1989) 824.
11. J. C. EDELSTEIN, E. S. WACHMAN, L. K. CHENG, W. R. BOSENBERG and C. L. TANG, *Appl. Phys. Lett.* **56** (1988) 2111.
12. Q. ZHAO, F. P. SCHÄFER and S. SZATMARI, *Appl. Phys.* **B46** (1988) 139.
13. S. SZATMARI and F. P. SCHÄFER, *Appl. Phys. Lett.* **68** (1988) 196.
14. I. V. TOMOV, R. FEDOSEJEVS and A. A. OFFENBERGER, *IEEE J. Quantum Electron.* **QE-18** (1982) 2048.
15. C. LEUBNER, H. SCHEINGRABER and C. R. VIDAL, *Opt. Commun.* **36** (1981) 205.
16. D. ANDERSON, M. LISAK and T. REICHEL, *Phys. Rev.* **A38** (1988) 1618.
17. J. T. MANASSAH, M. A. MUSTAFA, R. R. ALFANO and P. P. HO, *Phys. Lett.* **113A** (1985) 242.
18. D. ANDERSON and M. LISAK, *Phys. Rev.* **A27** (1983) 1393.
19. A. A. RADZIG and B. M. SMIRNOV, 'Parameters of Atoms and Atomic Ions', 2nd ed. (Energoatomizdat, Moscow, 1986) p. 215.
20. G. PEACH, *Mem. R. Astron. Soc.* **71** (1967) 13.
21. Y. PRIOR, *IEEE J. Quantum Electron.* **QE-20** (1984) 27.
22. S. G. DINEV and A. A. DREISCHUH, *Opt. Quantum Electron.* **23** (1991) 91.
23. J. C. SCHAEFER and I. CHABAY, *Opt. Lett.* **4** (1979) 227.
24. D. L. WINDT, W. C. CASH, Jr., M. SCOTT, P. ARENDT, B. NEWMAN, R. F. FISHER, A. B. SCHWARTZLANDER, P. Z. TAKACS and J. M. PINNEO, *Appl. Opt.* **27** (1988) 279.
25. J. T. MANASSAH and M. A. MUSTAFA, *J. Opt. Soc. Amer.* **B6** (1989) 1253.
26. *Idem, Ibid.*, **B6** (1989) 1258.